

Comparison of Soil Modeling Strategies with Springs in Free Span Submarine Pipelines

Matheus A. Miranda¹, Eduardo N. Lages¹

¹ *Laboratory of Scientific Computing and Visualization, Center of Technology, Federal University of Alagoas
Av. Lourival Melo Mota s/n, Cidade Universitária, 57072-900, Maceió/Alagoas, Brazil
matheus.miranda@ctec.ufal.br, enl@ctec.ufal.br*

Abstract. The fatigue life of submarine pipelines is significantly influenced by structural parameters and environmental conditions to which they are exposed. Numerous studies have focused on modeling this issue using the Finite Element Method to determine frequencies and natural vibration modes. The models consist of pipeline sections, with some segments in free spans and others supported by soils that can be represented by contact surfaces or sets of springs constituting an elastic foundation. This work evaluates different strategies for representing soil stiffness using springs in a finite element model. Additionally, we investigate the incorporation of the solution for a semi-infinite beam on an elastic foundation to calculate the parameters of the modeled endpoints. We analyze different element lengths in a free spanning pipeline model to quantify the influence of various approaches on frequencies and natural vibration modes. Therefore, this work emphasizes the relevance of parametric studies in modeling submarine pipelines, with particular emphasis on accounting for soil stiffness.

Keywords: Submarine Pipelines, Finite Element Method, Soil Stiffness.

1 Introduction

The increase in oil and gas exploration in offshore regions has required increasingly complex subsea systems located in deep and ultra-deep waters. The transportation of a significant portion of produced hydrocarbons is carried out through extensive networks of rigid subsea pipelines, which, due to seabed irregularities, have unsupported sections known as free spans. According to Lima [1], throughout the service life of the pipelines, these free span sections are subjected to periodic environmental loads, such as those caused by currents and waves, which can trigger the phenomenon of vortex-induced vibrations (VIV), posing a risk to the pipeline's structural integrity due to fatigue.

The structural analysis of pipelines in free spans involves various geometric, operational, and environmental parameters. It consists of static analyses and the analysis of the frequencies and natural vibration modes. This analysis is typically conducted using computational programs that employ the Finite Element Method and is essential for fatigue analysis. One of the main references on this subject is the recommended practice DNV-RP-F105 [2], which provides criteria and guidelines for evaluating the dynamic response of pipelines in free spans due to the combined action of waves and currents.

The RP-F105 describes various types of problem modeling, ranging from the most realistic, incorporating realistic seabed models to simplified ones, where supported sections (shoulders) are considered flat or simply as supports at the span ends. Considering simplified models with flat shoulders, studies such as those by Oliveira [3] and Ribeiro [4] modeled these sections with linear springs constituting an uncoupled elastic foundation using commercial software. This type of modeling requires greater discretization of the supported sections as it disregards the coupling of springs in the rotational degrees of freedom of the pipeline elements.

Moreover, these models generally represent a segment for analysis, as modeling the entire pipeline length is impractical. Thus, boundary conditions such as second or third-degree supports are typically imposed at the ends to represent the pipeline's continuity.

Therefore, this work evaluates the influence on frequencies and natural vibration modes, considering different modeling strategies for the elastic foundation to represent the supported sections. Additionally, it investigates the incorporation of the semi-infinite beam problem solution to define the model's endpoints.

2 Numerical modeling

Figure 1 depicts the numerical model developed. This model consists of segments representing supported sections on elastic foundations and free span sections. Additionally, the model ends have boundary conditions that can be modeled in various ways.

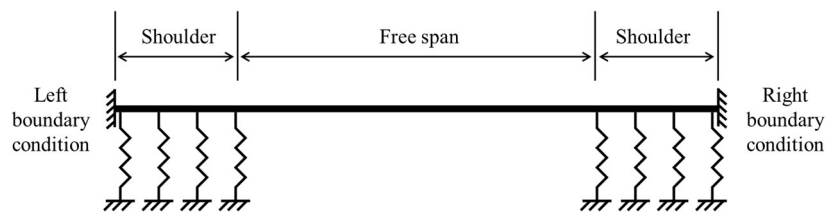


Figure 1. Numerical model representation

2.1 Pipeline

The pipeline is modeled using 2D frame elements, each containing 6 degrees of freedom, as shown in Fig. 2.

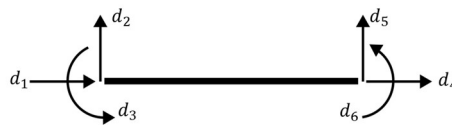


Figure 2. 2D frame element and degrees of freedom

These elements' mass and stiffness matrices are classical and detailed, e.g., in Paz and Kim's work [5]. It should be noted that rotational inertia contribution was disregarded in the mass matrix in this study.

2.2 Elastic foundation

Contributions from elastic foundations are added to the stiffness matrices of elements located in these regions to model the supported sections. In this study, two strategies were implemented.

The first strategy involves decoupled elastic foundations, where the stiffness of the springs contributes only to degrees of freedom along the directions where the springs are placed. The second strategy considers continuous elastic foundations, where there is a coupling between translational and rotational degrees of freedom. Axial and transverse stiffnesses were considered. The stiffness matrices for uncoupled (\mathbf{K}_U) and continuous (\mathbf{K}_C) elastic foundations can be derived considering strain energy and are, respectively, by eq. (1) and eq. (2), where k_a and k_t are the stiffnesses per unit length of the springs, and L_e is the element length.

$$\mathbf{K}_U = \begin{bmatrix} \frac{k_a L_e}{2} & 0 & 0 & 0 & 0 & 0 \\ 0 & \frac{k_t L_e}{2} & 0 & 0 & 0 & 0 \\ 0 & 0 & 0 & 0 & 0 & 0 \\ 0 & 0 & 0 & \frac{k_a L_e}{2} & 0 & 0 \\ 0 & 0 & 0 & 0 & \frac{k_t L_e}{2} & 0 \\ 0 & 0 & 0 & 0 & 0 & 0 \end{bmatrix}. \quad (1)$$

$$\mathbf{K}_C = \begin{bmatrix} \frac{k_a L_e}{3} & 0 & 0 & \frac{k_a L_e}{6} & 0 & 0 \\ 0 & \frac{13k_t L_e}{35} & \frac{11k_t L_e^2}{210} & 0 & \frac{9k_t L_e}{70} & -\frac{13k_t L_e^2}{420} \\ 0 & \frac{11k_t L_e^2}{210} & \frac{k_t L_e^3}{105} & 0 & \frac{13k_t L_e^2}{420} & -\frac{k_t L_e^3}{140} \\ \frac{k_a L_e}{6} & 0 & 0 & \frac{k_a L_e}{3} & 0 & 0 \\ 0 & \frac{9k_t L_e}{70} & \frac{13k_t L_e^2}{420} & 0 & \frac{13k_t L_e}{35} & -\frac{11k_t L_e^2}{210} \\ 0 & -\frac{13k_t L_e^2}{420} & -\frac{k_t L_e^3}{140} & 0 & -\frac{11k_t L_e^2}{210} & \frac{k_t L_e^3}{105} \end{bmatrix}. \quad (2)$$

2.3 Boundary conditions at modeled endpoints

The boundary conditions explored in this study were fixed supports and a condition associated with solving a semi-infinite beam problem on a continuous elastic foundation, depicted in Fig. 3.

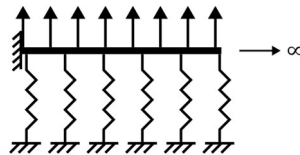


Figure. 3. The semi-infinite beam problem on a continuous elastic foundation

For the fixed support condition, solving the static problem and obtaining vibration modes can be achieved through recognized methods, such as partitioning of mass and stiffness matrices or penalty methods (see Fish and Belytschko [6]).

No rows and columns are eliminated from the global matrices for the boundary condition associated with the semi-infinite beam problem solution. Instead, their contributions are added to elements corresponding to the modeled endpoint nodes.

For example, the mass (\mathbf{M}_{SI}) and the stiffness (\mathbf{K}_{SI}) matrices presented in eq. (3) and eq. (4) should be added to the mass and stiffness matrices of the rightmost element of the model, where EA and EI are, respectively, axial and flexural stiffnesses, and ρ_a and ρ_t are linear densities (mass per unit length) in the axial and transverse directions.

$$\mathbf{M}_{SI} = \begin{bmatrix} 0 & 0 & 0 & 0 & 0 & 0 \\ 0 & 0 & 0 & 0 & 0 & 0 \\ 0 & 0 & 0 & 0 & 0 & 0 \\ 0 & 0 & 0 & \frac{\rho_a}{2} \sqrt{\frac{EA}{k_a}} & 0 & 0 \\ 0 & 0 & 0 & 0 & \frac{3\sqrt{2}\rho_t}{4} \left(\frac{EI}{k_t}\right)^{\frac{1}{4}} & \frac{\rho_t}{2} \sqrt{\frac{EI}{k_t}} \\ 0 & 0 & 0 & 0 & \frac{\rho_t}{2} \sqrt{\frac{EI}{k_t}} & \frac{\sqrt{2}\rho_t}{4} \left(\frac{EI}{k_t}\right)^{\frac{3}{4}} \end{bmatrix} \quad (3)$$

$$\mathbf{K}_{SI} = \begin{bmatrix} 0 & 0 & 0 & 0 & 0 & 0 \\ 0 & 0 & 0 & 0 & 0 & 0 \\ 0 & 0 & 0 & 0 & 0 & 0 \\ 0 & 0 & 0 & \frac{\sqrt{k_a EA}}{2} & 0 & 0 \\ 0 & 0 & 0 & 0 & \frac{(EI)^{\frac{1}{4}} k_t^{\frac{3}{4}} \sqrt{2}}{4} & \frac{\sqrt{k_t EI}}{2} \\ 0 & 0 & 0 & 0 & \frac{\sqrt{k_t EI}}{2} & \frac{3(EI)^{\frac{3}{4}} k_t^{\frac{1}{4}} \sqrt{2}}{4} \end{bmatrix} \quad (4)$$

2.4 Analysis steps

The analysis implemented in this study consists of two main steps:

- A static step where the submerged weight of the pipeline is applied, causing vertical displacements that are considered for calculating exposed and buried areas. These areas calculate additional mass to compose the mass matrix used in the subsequent step.
- A step for extracting frequencies and natural vibration modes, where the generalized eigenvector problem is solved with the stiffness matrix obtained in the static step and with the mass matrix calculated incorporating the additional mass due to changes in the pipeline configuration. It is worth noting that the stiffness matrix is not updated in the second step, as the springs are considered to behave linearly.

3 Study cases

This study conducted two case studies, which are presented in this section. Oliveira [3] obtained some shared data between the two studies listed in Tab. 1.

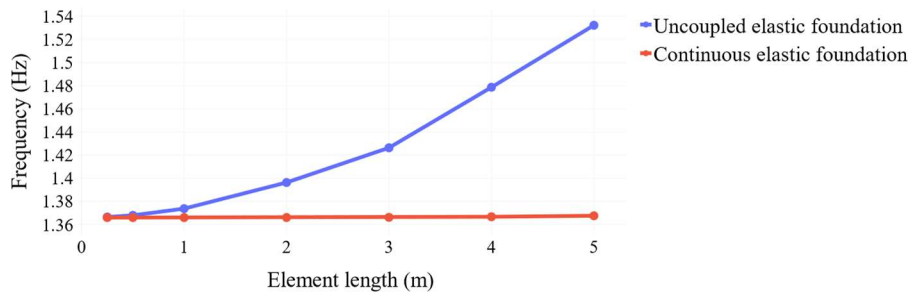
In addition to the data in Tab. 1, all models used for the studies feature two equally long supported sections and a central free span, as illustrated in Fig. 1.

Table 1. Data adopted in the case studies

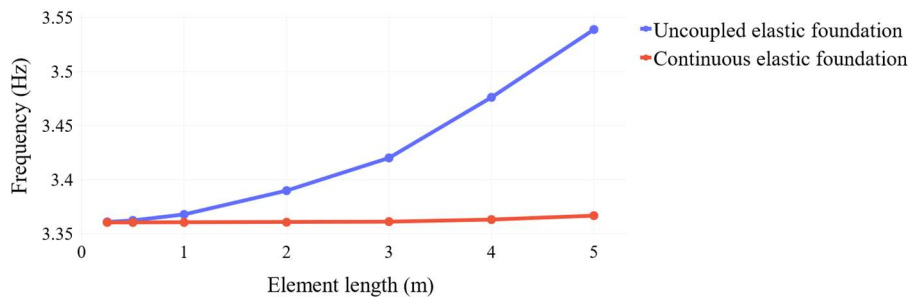
Parameter	Value	Unit
Outer steel diameter	0.27305	m
Wall thickness	0.0127	m
Young modulus	206.0	GPa
Poisson's ratio	0.29	-
Steel density	7850.0	kg/m ³
Water density	1025.0	kg/m ³
Soil density	1500.0	kg/m ³
Content density	200.0	kg/m ³
Inertia coefficient - axial direction	0.1	-
Inertia coefficient - transversal direction	1.0	-
Axial soil stiffness	160.0	kN/m/m
Transversal soil stiffness	160.0	kN/m/m

3.1 Comparison between the modeling approaches of the elastic foundation

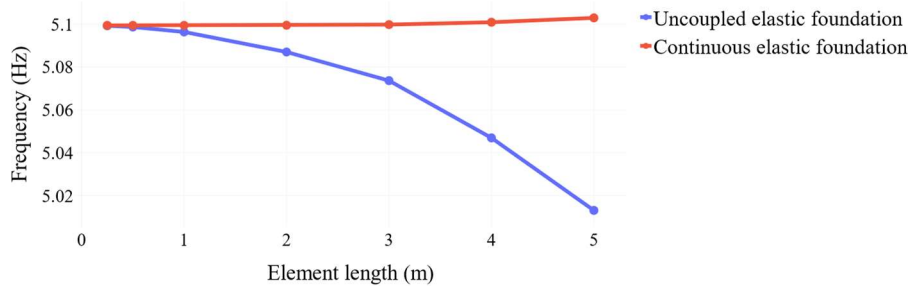
In this study, two models with the same geometric configuration were compared. The difference between the two models lies in the type of modeled elastic foundation, with the first model having a decoupled foundation and the second model having a continuous foundation. To conduct the study, various element lengths were used to assess the difference in each model's first three natural vibration frequencies. The results of this investigation are presented in Fig. 4.



a. First natural frequency



b. Second natural frequency



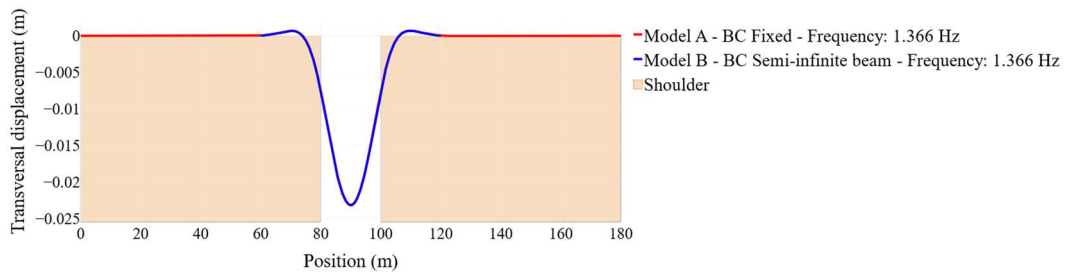
c. Third natural frequency

Figure 4. Results of the investigation for the first three natural vibration frequencies for models considering discontinuous and continuous elastic foundations

The study demonstrates that shorter element lengths yield similar frequencies, but longer lengths show significant differences between decoupled and continuous elastic foundation models. Continuous foundation modeling offers stable results with increased element length, proving computationally efficient for accurate structural analysis.

3.2 Investigation of the boundary condition associated with the solution of a semi-infinite beam supported on an elastic foundation

In this study, a model with long shoulder lengths using fixed boundary conditions at its ends (Model A) was compared with a model featuring shorter shoulders employing a boundary condition associated with the solution of a semi-infinite beam at the ends (Model B). The element length adopted for both models was 0.1 m, and the elastic foundation for both models was assumed to be continuous. Comparisons of the first two natural vibration modes for each model are presented in Fig. 5.



a. First vibration mode



b. Second vibration mode

Figure 5. Comparison of the first two natural vibration modes among models with distinct boundary conditions

It is observed that the vibration modes of Model B closely approached those of Model A. Thus, using the shorter model, which requires fewer computational resources, equivalent natural vibration modes, and frequencies were achieved compared to the more complex and costly model.

4 Conclusions

The importance of studying different strategies for numerically modeling free span pipelines becomes evident. Comparing discontinuous and continuous elastic foundation models showed consistent results with the latter approach as element lengths increased. Investigating a boundary condition based on a semi-infinite beam on an elastic foundation yielded comparable results to a more extensive model with fixed boundary conditions. These findings enable cost-effective computational modeling of free span pipeline scenarios without sacrificing accuracy.

Acknowledgements. This work was supported by the Federal University of Alagoas (UFAL), Coordination for the Improvement of Higher Education Personnel (CAPES), and the National Council for Scientific and Technological Development (CNPq).

Authorship statement. The authors hereby confirm that they are the sole liable persons responsible for the authorship of this work, and that all material that has been herein included as part of the present paper is either the property (and authorship) of the authors, or has the permission of the owners to be included here.

References

- [1] Lima, A. J. Análise de dutos submarinos sujeitos a vibrações induzidas por vórtices. Dissertação de Mestrado. COPPE/UFRJ, Rio de Janeiro, RJ, Brasil. 2007
- [2] DNV. DNV-RP-F105 Free spanning pipelines. 2017
- [3] Oliveira, A. E. C. Vibração de dutos submarinos com apoio em fundação elástica descontínua. Dissertação de Mestrado, PUC-Rio, Rio de Janeiro, RJ, Brasil. 2016.
- [4] Ribeiro, R. M. Comparação entre metodologias para recomendação de vão livre admissível em dutos rígidos submarinos. Dissertação de Mestrado. COPPE/UFRJ, Rio de Janeiro, RJ, Brasil. 2017.
- [5] Paz, M. and Kim, Y. H. Structural dynamics: Theory and computation. 2019.
- [6] Fish, J. and Belytschko, T. A First Course in Finite Elements. John Wiley & Sons Ltd, 2007.